Measurement of the photoionization cross section of the $5S_{1/2}$ state of rubidium

J. R. Lowell, T. Northup, B. M. Patterson, T. Takekoshi, and R. J. Knize
Laser and Optics Research Center, Department of Physics, United States Air Force Academy, Colorado Springs, Colorado 80840
(Received 23 April 2002; published 13 December 2002)

We report the measurement of the photoionization cross section for the $5S_{1/2}$ state of rubidium, using atoms confined in a magneto-optical trap. A single-photon rate at $\lambda = 266$ nm was found by monitoring the decay of trap fluorescence after exposure to ionizing radiation from a quadrupled Nd:YVO_4 laser. In order to eliminate excited-state ionization, the photoionization and trapping lasers were alternately chopped, so that only ground-state atoms were ionized. We determine that the photoionization cross section at $\lambda = 266$ nm is $\sigma = 1.7(2) \times 10^{-20}$ cm^2.

DOI: 10.1103/PhysRevA.66.062704 PACS number(s): 32.80.Fb, 32.80.Pj

I. INTRODUCTION

Photoionization of atoms from the ground state is an important process in many atomic, molecular, plasma, and astrophysical phenomena. Photoionization is the inverse of radiative recombination, which is also important in plasma physics. Measurements of photoionization cross sections can be used to test atomic theory. More recently, photoionization has been used to detect trapped atoms and molecules [1]. Since both atoms and molecules are photoionized in the trap, it is important to know both the atomic and molecular cross sections.

The first absolute photoionization cross-section measurements of ground-state rubidium atoms were made by Mohler and Boeckner [2] in 1929. The measurements were made using a space-charge amplification method in an ionization chamber to measure the photoionization cross section between 235 and 305 nm. Marr and Creek [3] extended this range to 120 nm, measuring the attenuation of photoionizing light in an atomic beam. In both experiments, the considerable fraction of Rb_2 molecules ($f_{\mathrm{mol}} \sim 0.3\%$) present may have affected the measurements [4]. The 1929 measurement could not discriminate between atomic and molecular photoionization, although the latter cross section may be 2 orders of magnitude greater at points in the spectrum [5]. The 1968 measurement relied on the linear relationship between absorption and pressure; however, this method requires an accurate knowledge of atomic and molecular vapor pressures. A 1983 survey [4] found determination of absolute cross sections was difficult using the reported data due to Rb density uncertainties of 10–80 % for a given temperature.

Additionally, there have been several theoretical calculations of photoionization cross sections, including *ab initio* calculations [6,7] and semiempirical calculations [8–11]. The principal experimental and theoretical results are tabulated in Table I.

Dinneen *et al.* [12] reported a method for measuring photoionization cross sections of cold, trapped, excited atoms. Rubidium atoms in the $5P_{3/2}$ state confined within a magneto-optical trap (MOT) were exposed to ionizing radiation and a subsequent decrease in the trap fluorescence measured to determine the absolute cross section. Subsequent measurements have employed similar trap loss techniques to measure cross sections of excited *P* and *D* states of Rb, Cs, and Mg [13–16]. This work will use a variation of this technique, in which we report measurement of the ground-state photoionization cross section by alternately chopping the trapping and ionizing radiation incident on the MOT.

II. EXPERIMENT

In this paper, we present the measurements of the photoionization cross section of the $5S_{1/2}$ state of ^{85}Rb using a MOT. Contrary to the vapor cell and atomic beam experiments outlined above, a MOT consists almost entirely of atoms (i.e., $f_{mol} \ll 0.3\%$) [17]. As described below, the cross section is determined from the time decay of the MOT fluorescence, which is a result of *atomic* excitation to the $5P_{3/2}$ state. As such, even if molecules are present in the MOT, the fluorescence measurement will be unaffected. Finally, the cross section is determined by looking at the time decay of the MOT fluorescence, therefore measurement of the atomic density or calibration of ion detection efficiency is not required.

The experiment was conducted in a vapor-loaded

TABLE I. A summary of previous ground-state cross-section measurements and theoretical calculations for ^{85}Rb.

Work	σ (10^{-20} cm^2)	Uncertainty (%)
Experiment [2]	1.8[a]	50[b]
Experiment [c]	1.2[a]	50[b]
Experiment [3]	1.9	20+10 [d]
Experiment [e]	1.5	20+10 [d]
Current work	1.7	12
Ab initio [6]	4 [a]	
Ab initio [7]	0.7[a]	
Semiempirical [9]	1.3	

[a]Inferred from plot.
[b]Uncertainty estimated from inability to differentiate Rb_2 from Rb.
[c]Mohler and Boeckner's work rescaled by Marr and Creek [3].
[d]The 20% error is inferred from error bars at 248 and 297 nm. The 10% is a minimum estimate of the systematic error from use of a vapor pressure table; this could be as high as 80%.
[e]Marr and Creek's rescaled by Suemitsu and Samson [4].

magneto-optical trap, contained in a stainless-steel vacuum chamber maintained at a background pressure of about 10^{-9} Torr. The vacuum chamber had six orthogonal optical viewports, through which the circularly polarized trapping lasers passed. It also had additional viewports beyond those on the trapping axes, including one for a photodiode to measure MOT fluorescence, one for a camera, and one with a quartz window with a power transmission of $T=89\%\pm3\%$ at $\lambda_P=266$ nm, through which the UV photoionizing beam was sent.

The trapping laser was a temperature-stabilized diode laser in an external cavity configuration [18], frequency locked approximately 2.3 natural linewidths (13.8 MHz) below the $F=3\rightarrow4$ trapping transition. The MOT trapping beams were spatially filtered through a fiber, expanded to 2 cm in diameter, and produced a maximum total MOT intensity of 8.5 mW/cm^2 in the six MOT beams. A separate temperature-stabilized, frequency-locked diode laser in the external cavity configuration provided 0.2 mW/cm^2 for the $F=2\rightarrow3$ repumping transition. An axial magnetic-field gradient of 12.5 G/cm was maintained throughout the experiment, resulting in a trap with radius 170 μm. The trap lifetime was $\tau_{\mathrm{trap}}=3.5\pm0.3$ s, which was limited by background gas collisions.

The UV ionizing radiation was produced by a Coherent Verdi (a doubled Nd:YVO_4 laser) passed through a Coherent model MBD-266 frequency doubler. The UV laser output was continuous, so an optical chopping wheel was placed in the light path. By passing the UV beam through a mechanical shutter and a chopping wheel (twice), 275 μs pulses at a 1000 Hz frequency were incident on the MOT. The UV pulse length could be varied from 40 μs to about 290 μs, and no significant change was observed in the photoionization cross section as this value was changed. All reported measurements were conducted with a UV pulse duration of 275 μs.

In order to ensure only cold ground-state rubidium atoms were present during exposure to the UV photoionization radiation, the trapping (and repumping) beams were shut off using an acousto-optical modulator (AOM) approximately 45 μs before exposure to the UV light. We installed additional switches to ensure no residual rf power was incident at the AOM crystals when we turned the rf drivers off. The trapping beams were turned back on approximately 45 μs after shuttering off the UV radiation, giving a 365 μs shutter width for the trapping beams. The timing of the trapping and photoionization beams is shown in Fig. 1.

The lifetime of the $5P_{3/2}$ state in Rb is 27 ns. For a typical 45 μs delay between the extinction of the trapping lasers and the arrival of the UV photoionization pulse, the excited-state population fraction f solely due to spontaneous decay from the $5P_{3/2}$ state is $f\approx10^{-644}$. At room temperature, the excited-state population fraction is expected to be $f\approx10^{-27}$. Clearly, neither of these contribute any population into the excited-state. Any significant excited-state population must therefore arise from optical pumping into the $5P_{3/2}$ state. We make two measurements of this fraction: first, we measured photoionization rate using a 473 nm laser while the MOT beams were shuttered off with the AOMs [19]; and second, we measure how much of the trapping laser light is

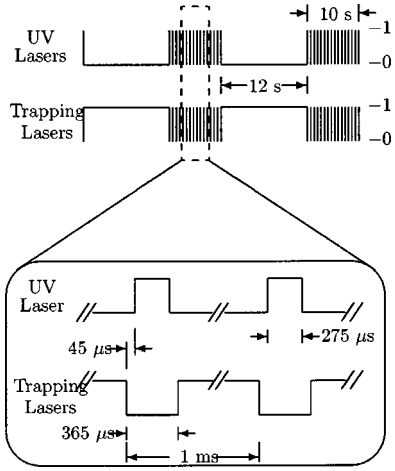

FIG. 1. Typical timing sequence for the trapping lasers (the repumping laser is shut off identically to the trapping lasers) and the photoionization laser. The top sequence shows the coarse timing, in which the trapping lasers are on and the UV laser is off to allow the trap to load. The inset shows the detailed timing sequence for the shuttering of the trapping and UV lasers to ensure photoionization of the ground-state atoms.

incident on the MOT when the AOM shutter is closed. The first measurement gives an upper limit of $f<5\times10^{-6}$. Since the excited-state photoionization cross section at $\lambda_P=266$ nm is about 10^{-17} cm^2 [20], this limit indicates a contribution of less than 10^{-4} to the collected signal.

The ratio of leaked power when the shutter is closed to passed power when the shutter is open (extinction ratio) through the AOM was measured to be less than 5×10^{-6}, which accounts for scattering losses in the beam transmission optics, and ambient leakage into the vacuum chamber from that scattered light. Thus, the intensity of the resonant light incident on the MOT is $I<1.4$ nW/cm^2 with the AOM shutter closed. Using the method of Javanainen [21] with the notation of Patterson *et al.* [14], we calculate the excited-state fraction in the MOT as

$$f=\frac{\left(\frac{I}{I_S^\delta}\right)}{2\left(\frac{I}{I_S^\delta}\right)+1}, \tag{1}$$

where I is the incident intensity and I_S^δ is the saturation intensity at the detuning δ, given by

$$I_S^\delta=I_S\left[\left(\frac{2\delta}{\Gamma}\right)+1\right]. \tag{2}$$

I_S is the saturation intensity at zero detuning, which is 4.44 mW/cm^2 in Rb. At our detuning, $I_S^\delta=24.8$ mW/cm^2, giving us an excited-state fraction of $f<1\times10^{-5}$ at the start of the UV photoionization pulse, implying a contribution of

less than 10^{-3} (0.1%) to the collected signal. Both estimates of the excited-state fraction give a contribution to the photoionization rate of less than 10^{-3} (0.1%). This ensures, we are only measuring ground-state photoionization.

The photoionization rates were determined by detecting the decay in trap fluorescence after the UV laser was shuttered on. The trap fluorescence was focused onto a diode photodetector. Unwanted light was blocked using an interference optical filter placed just in front of the photodetector. The interference filter has an optical density at λ_P greater than 4 (OD$>$4), whereas the transmission coefficient at 780 nm is approximately 80%, ensuring that we are only measuring trap fluorescence and not the UV laser. The trap fluorescence was recorded as a function of time both with and without ionizing radiation present, that is, both trap decay and growth curves were collected consecutively. Data were sampled at 10^4 Hz, passed through an amplifier (which also acted as a 100 Hz low-pass filter). Each data acquisition involved the averaging of eight consecutive trials, each of which contained a pair of 10 s measurements of trap decay (UV on) and growth (UV off).

III. THEORY AND ANALYSIS

The number of atoms contained in a MOT (denoted here as N) is determined by a combination of several characteristics, principally the collisional loss rate (R_L) and the atom capture rate (Γ_c). In a vapor-loaded MOT such as ours, the collisional loss rate will be dominated by collisions between cold-trapped atoms and the hot atoms in the background gas. The atom capture rate is dependent on the density of background gas atoms in the capture volume of the trapping beams.

The presence of photoionizing radiation will alter the normal balance between Γ_c and R_L, in a manner that depends on the photoionization rate (R_P), such that the rate of change in the number of atoms in the MOT is given by

$$\frac{dN}{dt}=\Gamma_c-(R_L+R_P)N=\Gamma_c-R_TN, \tag{3}$$

where we denote the total trap loss rate due to both collisions and photoionization as $R_T=R_L+R_P$. The equilibrium number of trapped atoms will therefore shift from $N_0=\Gamma_c(R_L)^{-1}$ to $N_0'=\Gamma_c'(R_T)^{-1}$ in the presence of ionizing radiation (the modified atom capture rate accounts for the presence of ionizing radiation in the trapping volume). The solutions of Eq. (3) will then assume the forms

$$N(t)=N_0'+(N_0-N_0')e^{-(R_T)t} \tag{4}$$

and

$$N(t)=N_0-(N_0-N_0')e^{-(R_L)t}, \tag{5}$$

for trap decay in the presence of ionizing radiation and trap growth in the absence of ionizing radiation, respectively.

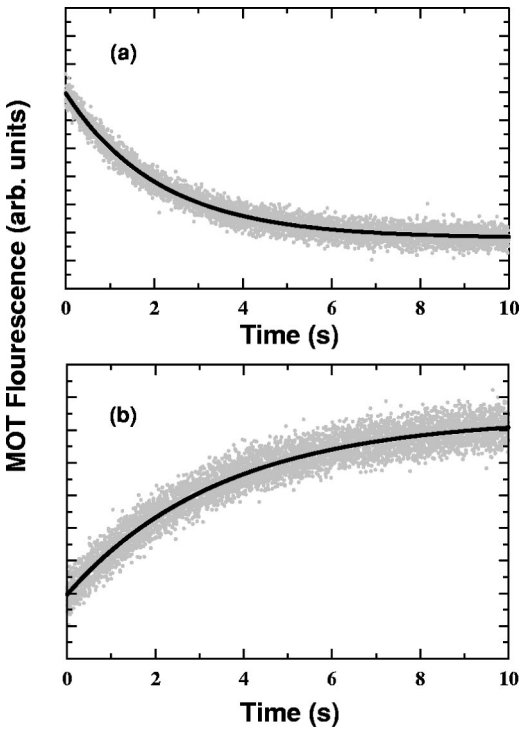

FIG. 2. Typical fluorescence data as a function of time acquired (a) with the UV ionization laser on (MOT decay), and (b) during loading, after the UV ionization laser was turned off. The data are indicated by gray points, while the solid lines indicate the best-fit curves through the data. Only every other data point is plotted. The fits to Eqs. (4) and (5) give characteristic decay and growth rates of $R_T=0.47\ \mathrm{s}^{-1}$ and $R_L=0.29\ \mathrm{s}^{-1}$, respectively.

A. Determination of R_P

To account for any potential drift in the collisional loss rate from experiment to experiment, photoionization decay and MOT loading curves were acquired sequentially. The photoionization rate R_P was determined by the difference in the decay and loading rates of these successive measurements. Figure 2 shows a typical set of decay and growth curves. The decay and growth data were independently fit to the functions of Eqs. (4) and (5), giving decay and growth rates of $R_T=0.47\ \mathrm{s}^{-1}$ and $R_L=0.29\ \mathrm{s}^{-1}$, respectively. The resulting photoionization rate is therefore $R_P=0.18\ \mathrm{s}^{-1}$ for these data.

These measurements were repeated at a variety of UV photoionization laser powers (or intensities) to ensure that we were not saturating the ionization process. The results of these measurements are shown in Fig. 3. A weighted linear fit to the data indicates that $R_P/P=4.2(2)\ \mathrm{J}^{-1}$, and that we are far from saturating the photoionization transition. In these measurements the UV power P is the average power after the chopper.

B. Determination of σ

The photoionization cross section σ is determined from the photoionization rate R_P and the characteristics of both the UV laser and the MOT. When the intensity of the ionizing radiation is well below the saturation intensity, as we have shown to be the case, the photoionization cross section is given by

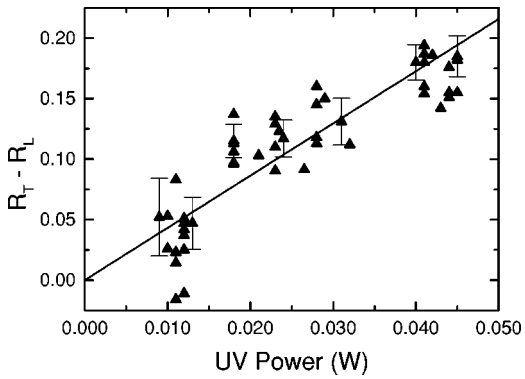

FIG. 3. Photoionization rate measurements (▲) plotted as a function of UV laser power incident on the vacuum chamber. The solid line (—) is a weighted least-squares fit to a line passing through the origin, with a slope of $R_P/P=4.2(2)\ \mathrm{J}^{-1}$. The fitting weights are assigned to the data points in several groups, based on the uncertainty of the measurements made in each group. The uncertainty for each group is represented by an error bar on one of the data points.

$$\sigma=\frac{R_P(h\nu)}{\overline{I_P}}, \tag{6}$$

where $h\nu$ is the energy of the ionizing photon, $\overline{I_P}$ is the average intensity of the photoionization beam seen by the atoms in the MOT, and R_P is the measured photoionization rate. The average intensity seen by the atoms will depend on UV laser power and beam size, MOT size, how well the UV laser is overlapped with the MOT, and the window transmission.

To measure the intensity of the UV ionizing radiation, we determined the UV beam profile using a knife-edge measurement. The beam was an elliptical Gaussian beam, with e^{-2} half waists of $\sigma_x=425(2)\ \mu$m and $\sigma_y=631(3)\ \mu$m at the location of the MOT (2.5–3.5 times the size of the MOT). For such a beam, the peak intensity I_0 seen by the atoms in the MOT is

$$I_0=\frac{2(PT)}{\pi\sigma_x\sigma_y}, \tag{7}$$

where P is the power incident on the vacuum chamber and T is the power transmission coefficient of the quartz window [22]. The intensity distribution is given by

$$I(x,y)=I_0\exp\left[-\frac{2x^2}{\sigma_x^2}\right]\exp\left[-\frac{2y^2}{\sigma_y^2}\right]. \tag{8}$$

We find the average intensity seen by the atoms by averaging this intensity distribution with the spatial distribution of the trapped atoms projected onto a plane normal to the UV beam propagation. We measured the spatial distribution of the trapped atoms by imaging the photons emitted by the MOT onto a charge-coupled device camera. Several measurements of the two-dimensional profile of the MOT indicate that the atoms are distributed as

$$N(x,y)=\frac{2N_0}{\pi s^2}\exp\left[-\frac{2(x^2+y^2)}{s^2}\right], \tag{9}$$

where N_0 is the total number of atoms in the MOT, and $s=170\ \mu$m is the e^{-2} radius of the trap. Defining the fractional distribution of atoms as $n(x,y)=N(x,y)/N_0$, we can write the average intensity of the ionization laser seen by an atom in the MOT as

$$\overline{I_P}=\int_{-\infty}^{\infty}\int_{-\infty}^{\infty}I(x,y)n(x,y)dxdy=\frac{2I_0}{s^2}\sqrt{\frac{1}{ab}}. \tag{10}$$

We have used the notation here that

$$a=\frac{2}{s^2}+\frac{2}{\sigma_x^2},$$

$$b=\frac{2}{s^2}+\frac{2}{\sigma_y^2}.$$

For the parameters given above, we calculate the average intensity seen by the atoms to be

$$\eta=\frac{\overline{I_P}}{I_0}=89\%$$

of the peak intensity in the UV beam. Putting all this together, we can rewrite Eq. (6) as

$$\sigma=(h\nu)\left(\frac{R_P}{P}\right)\left(\frac{\pi\sigma_x\sigma_y}{2T\eta}\right). \tag{11}$$

The first factor in this equation is the energy of the photon, the factor R_P/P is the slope of the best-fit line in Fig. 3, and the last factor is due to the geometry of our experiment.

C. Sources of uncertainty and conclusions

In Eq. (11), there are several potential sources of uncertainty in the measurement of the cross section. Measured uncertainty in the power transmission of the UV window at 266 nm is about 3%. We measured the uncertainty in the factor η to be approximately 5% by looking at the scatter in the excited-state fluorescence seen when the UV laser was overlapped with the trap. The absolute UV power measurement has an estimated uncertainty of about 8%. Errors that are less than 1% include: uncertainties in the UV beam profiles, MOT size, and UV laser frequency drift. The statistical error from the fit is about 5%. From the measurements and Eq. (11), we determine that the photoionization cross section at $\lambda=266$ nm is $\sigma=1.7(2)\times10^{-20}\ \mathrm{cm}^2$. This result is in agreement with previous measurements and is a factor of 2–4 times more accurate. It is not in good agreement with the semiempirical calculation or the two *ab initio* theories.

In conclusion, we have made a measurement of the

ground-state photoionization cross section of Rb using a magneto-optical trap. The technique requires no measurement of the atomic (or molecular) density or calibration of ion detection efficiency; it relies instead on monitoring the time decay of trap fluorescence in the presence and absence of photoionizing radiation. The single-photon cross section at $\lambda = 266$ nm was found to be $\sigma = 1.7(2) \times 10^{-20}$ cm^2.

ACKNOWLEDGMENTS

This work has been supported by funding from the U.S. Air Force Office of Scientific Research and the National Science Foundation. The authors would also like to acknowledge the generous support of the Department of Physics and the Dean of Faculty at the United States Air Force Academy.

[1] T. Takekoshi, B.M. Patterson, and R.J. Knize, Phys. Rev. A **59**, R5 (1999).
[2] F.L. Mohler and C. Boeckner, J. Res. Natl. Bur. Stand. **3**, 303 (1929).
[3] G.V. Marr and D.M. Creek, Proc. R. Soc. London, Ser. A **304**, 233 (1968).
[4] H. Suemitsu and J.A.R. Samson, Phys. Rev. A **28**, 2752 (1983).
[5] D.M. Creek and G.V. Marr, J. Quant. Spectrosc. Radiat. Transf. **8**, 1431 (1968).
[6] J.-J. Chang and H.P. Kelly, Phys. Rev. A **5**, 1713 (1972).
[7] M.G.J. Fink and W.R. Johnson, Phys. Rev. A **34**, 3754 (1986).
[8] I.D. Petrov, V.L. Sukhorukov, and H. Hotop, J. Phys. B **32**, 973 (1999).
[9] J.C. Weisheit, Phys. Rev. A **5**, 1621 (1972).
[10] F. Fuso, D. Ciampini, E. Arimondo, and C. Gabbanini, Opt. Commun. **144**, 173 (2000).
[11] I.D. Petrov, V.L. Sukhorukov, E. Leber, and H. Hotop, Eur. Phys. J. D **10**, 53 (2000).
[12] T.P. Dinneen, C.D. Wallace, K.-Y.N. Tan, and P.L. Gould, Opt. Lett. **17**, 1706 (1992).
[13] C. Gabbanini, S. Gozzini, and A. Lucchesini, Opt. Commun. **141**, 25 (1997).
[14] B.M. Patterson, T. Takekoshi, and R.J. Knize, Phys. Rev. A **59**, 2508 (1999).
[15] O. Maragò, D. Ciampini, F. Fuso, E. Arimondo, C. Babbanini, and S.T. Manson, Phys. Rev. A **57**, R4110 (1998).
[16] B.C. Duncan, V. Sanchez-Villicana, P.L. Gould, and H.R. Sadeghpour, Phys. Rev. A **63**, 043411 (2001).
[17] T. Takekoshi, B.M. Patterson, and R.J. Knize, Phys. Rev. Lett. **81**, 5105 (1998).
[18] K.B. MacAdam, A. Steinbach, and C.E. Wieman, Am. J. Phys. **60**, 1098 (1992).
[19] T. Northup, J.R. Lowell, B.M. Patterson, T. Takekoshi, and R.J. Knize (unpublished).
[20] M. Aymar, O. Robaux, and S. Wane, J. Phys. B **17**, 993 (1984).
[21] J. Javanainen, J. Opt. Soc. Am. B **10**, 572 (1993).
[22] P.W. Milonni and J.H. Eberly, *Lasers* (Wiley-Interscience, New York, 1988).